Using Energy Shaping and Regulation for Limit Cycle Stabilization, Generation, and Transition in Simple Locomotive Systems

Mark Yeatman
Student Member of ASME
Department of Mechanical Engineering
University of Texas at Dallas

Robert D. Gregg *
Department of Electrical Engineering and Computer Science
University of Michigan
Email: rdgregg@umich.edu

This paper explores new ways to use energy shaping and regulation methods in walking systems to generate new passive-like gaits and dynamically transition between them. We recapitulate a control framework for Lagrangian hybrid systems, and show that regulating a state varying energy function is equivalent to applying energy shaping and regulating the system to a constant energy value. We then consider a simple 1-dimensional hopping robot and show how energy shaping and regulation control can be used to generate and transition between nearly globally stable hopping limit cycles. The principles from this example are then applied on two canonical walking models, the spring loaded inverted pendulum (SLIP) and compass gait biped, to generate and transition between locomotive gaits. These examples show that piecewise jumps in control parameters can be used to achieve stable changes in desired gait characteristics dynamically/online.

1 Introduction

Research for creating periodic gaits in locomotive systems has been in development since the early 2000's, with a celebrated example of Hybrid Zero Dynamics (HZD) [1, 2]. This methodology revolves around designing state output functions via Bezier polynomials such that when they are driven to zero, a robot achieves a walking gait with predefined trajectories. More recent work has focused on extending HZD to achieve dynamic motion transition through motion planning techniques [3–5]. A trajectory-free method that contrasts HZD is to mimic and stabilize "natural" or passive dynamic walking gaits through "energy shaping", a termed coined in works on Interconnection and Damping Assignment Passivity-Based Control (IDA-PBC) [6, 7] and Controlled Lagrangian [8, 9] techniques. The general equivalence between passivity-based energy shaping and other techniques has been demonstrated, such as "Controlled Hamiltonian" [10] or "Immersion and Invariance" [11]. Energy shaping methods have a focus on using physically meaningful parameters to produce desired system properties, which can provide intuition in the analysis and design of extremely nonlinear systems in ways other control methods cannot, such as generalization of stability margins [12]. As seen in [13–16], energy shaping can force a biped robot to emulate the dynamics of a target passive locomotive system, then exploit a passivity property between the input and energy-based output to regulate the desired energy level associated with a limit cycle without canceling the nonlinear dynamics. Our paper is in this vein, but expands upon these previous works by dynamically transitioning between gaits through online switching of both the target energy and the system parameters of the emulated locomotive system. This offers a more simple (and arguably more natural) procedure for achieving *dynamic gait transition* than designing a plethora of gait trajectories and the transitions between them.

Inspired by [7] and [13] , our approach to generate limit cycles is as follows. First, identify a target Lagrangian system endowed with a continuum of periodic orbits where each orbit is associated with a unique energy value, and then set the control equal to the difference between the open-loop system dynamics and the desired system dynamics. This forces the closed-loop system to behave like the desired system. We refer to this step as energy shaping. Second, use an outer-loop controller to target a specific orbit by driving the system to the associated energy level set, creating a self-sustaining oscillator. We refer to this technique as en-

*Corresponding Author

ergy regulation. Ideally, this would allow us to switch between orbits by changing just the target system energy. For walking systems it is not quite that simple because hybrid dynamics with dissipative impact maps can cause limit cycles, which by definition preclude other nearby periodic orbits [17]. However, changes in the system parameters, like mass and gravity, can result in changes in the limit cycle trajectory. Thus, we will modify both the virtual system parameters and target reference energy to generate and transition between new limit cycles (essentially the idea of Lyapunov funneling [18, 19]).

Our paper extends and connects the work on the compass gait biped in [13] by Spong, Holm, and Lee and the spring based models in [15, 20] by Garofalo and Ott. The paper by Spong et al. uses "Controlled Symmetries", a form of energy shaping, to change the direction of the virtual gravity vector of the compass gait biped combined with an energy regulation technique to robustify walking gaits. The paper [20] by Garofalo et al. uses energy regulation techniques to control the hopping height of a springy robot, while [15] uses energy regulation in conjunction with an embedded SLIP controller on a walker with knees and a torso. One of the main differences between the SLIP and compass gait models is that the compass gait has energy dissipation at impact while the SLIP model does not, which plays a key role in the stability of their passive limit cycles. The consideration of both of these models is important because they are both fundamental to biped locomotion [21, 22]. We note that this idea of causing systems to emulate self sustaining nonlinear oscillators has connections outside the domain of walking bipeds; [23] is an example in the area micro-electro-mechanical-systems (MEMS) that uses feedback control to cause a microbeam to behave like a van-der-Pol or Rayleigh oscillator.

The primary contribution of this paper is an analytical framework and simulation results for the use of energy shaping and regulation to *dynamically transition* between a range of walking gaits on hybrid locomotive systems by leveraging relations between system parameters and desired limit cycle characteristics. Using this framework, we demonstrate an equivalence between regulation of a time/state-varying energy function and a 2-step process of energy shaping then energy regulation of a constant reference value. We then argue that regulating a constant energy value is the more meaningful and clear method of control construction because the asymptotic limit cycle trajectory is an energy level set of some system. We consider a simple hopping robot that illustrates the relationships between impact dissipation, system parameters, energy, and limit cycle behavior. This leads us to create a novel discrete update law for the reference energy that increases the robustness of a passive limit cycle in the face of parameter uncertainty. We apply this law to the compass gait biped in simulation, which is useful because the energy associated with a limit cycle cannot be analytically computed in this model. The difference between this work and [13] is that we change the virtual mass instead of gravity. Changing the virtual mass does not enjoy the same "Controlled Symmetry" property and is fundamentally more difficult to analyze. A strict extension of [13] in this paper is that we *dynamically transition* between different walking gaits on the compass gait biped using the energy regulation technique. In the same vein, our paper extends work on the SLIP model in [15, 20] by accomplishing dynamic gait transitions through switches in the target energy and spring stiffness. Finally, we also explicitly demonstrate that energy regulation can stabilize unstable limit cycles on the compass gait biped.

The organization of the paper is as follows: Section 2 of the paper gives a brief review of hybrid Lagrangian dynamics with impacts and the application of energy shaping and regulation to this class of systems. Section 3 details the dynamics and control of a hopping robot to illustrate concepts. Section 4 presents the SLIP model dynamics, control, and simulations that transition between various running speeds. Section 5 presents the compass gait biped model dynamics, control, and simulations that transition between walking speeds and stabilize previously unstable limit cycles of the passive system.

Notation: Given two matrices a and b of suitable dimensions, the matrix $[a^\top, b^\top]^\top$ is denoted by $[a;b]$ where $\top$ is the transpose operator.

Remark 1. *In this paper, it is important to distinguish between the terms "passive" versus "passivity" and the concepts to which they refer. To be clear, the term "passive" refers to an uncontrolled mechanical system composed of connected masses, springs, and dampers. The term "passivity" refers to the following mathematical definition.*

Definition 1. *Let $S(q,\dot{q}) : \mathbb{R}^{2n} \to \mathbb{R}$ be a continuously differentiable, non-negative scalar function. A system $[\dot{q};\ddot{q}] = f([q;\dot{q}]) + g([q;\dot{q}])u, \gamma = \eta([q;\dot{q}])$ has a passivity relationship between input u and output γ with storage function $S(q,\dot{q})$ if $\dot{S}(q,\dot{q}) \leq u^\top \gamma$.*

2 Energy Shaping and Regulation with Lagrangian Dynamics

There are many papers on the idea of energy shaping control for mechanical systems (which can be described by Lagrangian or Hamiltonian dynamics); seminal work in this area includes "Controlled Lagrangians" by Bloch et al. in [8] and "Interconnection and Damping Assignment Passivity-Based Control" by Ortega et al. in [6]. Recently, there has been a focus on using similar methods to stabilize periodic orbits, in both non-hybrid [7] and hybrid systems [16, 24]. We review some methods and notation to apply these techniques on hybrid systems with Lagrangian dynamics and impacts. The general idea is to first use energy shaping to generate desired virtual Lagrangian dynamics in the closed-loop, then use energy regulation to drive the associated virtual energy function to a desired reference value associated with a limit cycle.

2.1 Hybrid Lagrangian Dynamics

We begin by defining the general notation of hybrid Lagrangian dynamics with impacts. The state of the system is given by the vector $q \in \mathbb{R}^n$. The continuous dynamics can be derived from the Euler-Lagrange (EL) equations which have the following form:

$$\frac{d}{dt}\frac{\partial \mathcal{L}(q,\dot{q})}{\partial \dot{q}} - \frac{\partial \mathcal{L}(q,\dot{q})}{\partial q} = B(q)u. \tag{1}$$

The Lagrangian $\mathcal{L} = \mathcal{K}(q,\dot{q}) - \mathcal{P}(q)$ is the difference between the system's kinetic energy $\mathcal{K}$ and the potential energy $\mathcal{P}$. The external control forces $u \in \mathbb{R}^m$ are mapped into the dynamics by the matrix $B \in \mathbb{R}^{n\times m}$. Kinetic energy can be expressed as $\mathcal{K} = \frac{1}{2}\dot{q}^\top M(q)\dot{q}$, where $M(q)$ is a positive definite symmetric matrix that represents the mass/inertia of the system. The EL equations expressed in matrix form are

$$M(q)\ddot{q} + C(q,\dot{q})\dot{q} + G(q) = B(q)u \tag{2}$$

where the vector $C\dot{q}$ represents Coriolis and centripetal forces and the vector $G = \frac{\partial \mathcal{P}(q)}{\partial q}$ represents gravity. The matrix C is constructed such that $\dot{M} - 2C$ is skew symmetric.

Discrete impact dynamics capture the effect of system components coming in sudden contact with surfaces that constrain the motion of the system. The superscript notation $-$ and $+$ denotes variables just before and after impact, respectively. We define a switching surface $\mathbf{S}$ as

$$\mathbf{S} = \{(q,\dot{q}) \,|\, h(q^-) = 0, \dot{h} < 0\} \tag{3}$$

where the function h gives the distance of the system component from the constraint surface. The inequality $\dot{h} < 0$ ensures that the component is moving into the constraint before impact. The impact triggers when the state of system enters the switching surface. We use the impact model from [2] which causes instant, dissipative changes in the joint velocities of the system, but not the joint positions. However, we do allow the world frame to jump and the coordinates of the biped to be relabeled, which can appear as jumps in the position depending on the choice of coordinates. The impact map is denoted by $(q^+,\dot{q}^+) = \Delta(q^-,\dot{q}^-)$. The combination of the continuous and discrete dynamics results in hybrid Lagrangian dynamics with impacts, expressed as

$$B(q)u = M(q)\ddot{q} + C(q,\dot{q})\dot{q} + G(q) \quad \text{if} (q,\dot{q}) \notin \mathbf{S} \tag{4}$$

$$(q^+,\dot{q}^+) = \Delta(q^-,\dot{q}^-) \quad \text{if} (q,\dot{q}) \in \mathbf{S} \tag{5}$$

2.2 Energy Shaping and Regulation Control

Our control approach is partitioned into two parts $u = u_s + u_r$ so that u_s performs energy shaping and u_r performs energy regulation. The method of energy shaping we will use is that of Controlled Lagrangians [8]. We define a target mechanical system with Lagrangian $\widetilde{\mathcal{L}}$, derive target dynamics through the EL equations (1), and set the control equal to the difference between the open loop dynamics and the target dynamics. This yields the control law

$$u_s = (B^\top B)^{-1}B^\top(C\dot{q} + G - M\widetilde{M}^{-1}(\widetilde{C}\dot{q} + \widetilde{G})), \tag{6}$$

which will render the desired dynamics if and only if the so-called "matching condition"

$$B^\perp(C\dot{q} + G - M\widetilde{M}^{-1}(\widetilde{C}\dot{q} + \widetilde{G})) = 0, \tag{7}$$

is satisfied. Here, $B^\perp$ is a full rank left annihilator of B, i.e., $B^\perp B = 0$. The matching condition basically ensures there is never a component of the difference between the open-loop and desired dynamics in the nullspace of B. The new continuous dynamics are then

$$\widetilde{M}M^{-1}Bu_r = \widetilde{M}\ddot{q} + \widetilde{C}\dot{q} + \widetilde{G}. \tag{8}$$

2.2.1 Regulating a Constant Reference Energy

The energy of the new system can be regulated using the passivity-based control method from [13, 24] through the term u_r. Consider the following storage function (Definition 1)

$$S = \frac{1}{2}(\widetilde{E} - E_{\text{ref}})^2, \tag{9}$$

where $\widetilde{E}(q,\dot{q})$ is the closed-loop system energy and E_{ref} is the reference energy. The time derivative of this storage function is

$$\dot{S} = (\dot{\widetilde{E}} - \dot{E}_{\text{ref}})(\widetilde{E} - E_{\text{ref}}). \tag{10}$$

From the equation for the shaped dynamics (8),

$$\dot{\widetilde{E}} = \dot{q}^\top \widetilde{M}M^{-1}Bu_r \tag{11}$$

$$= \dot{q}^\top \widetilde{B}u_r. \tag{12}$$

If the reference energy is constant then $\dot{E}_{\text{ref}} = 0$ and

$$\dot{S} = \dot{q}^\top \widetilde{B}u_r(\widetilde{E} - E_{\text{ref}}). \tag{13}$$

Moreover, $\dot{S}$ can be rendered negative semi-definite by choosing

$$u_r = -\kappa(\widetilde{E} - E_{\text{ref}})\Omega\widetilde{B}^\top\dot{q}. \tag{14}$$

Here, $\kappa > 0$ is a scalar gain while the matrix $\Omega \in \mathbb{R}^{n\times n}$ is a positive definite weighting matrix with each element less

than one. The storage function and its derivative are related by

$$\dot{S} = -\kappa(\widetilde{E} - E_{\text{ref}})^2 \dot{q}^\top \widetilde{B}\Omega\widetilde{B}^\top \dot{q} \tag{15}$$

$$= -2\kappa||\dot{q}||_\Omega S, \tag{16}$$

where the term $\dot{q}^\top \widetilde{B}\Omega\widetilde{B}^\top \dot{q}$ is a norm. The convergence of the virtual energy to the target reference energy is guaranteed if the system state cannot enter some positively invariant set where $||\dot{q}||_\Omega = 0$ (LaSalle's invariance principle can be applied to validate this).

This controller differs from a similar method for Port-Hamiltonian systems in [7]; their control construction requires the ability to identify a state variable transformation that decomposes a limit cycle into a 2 dimensional submanifold where periodic motion occurs and a $n-2$ dimensional submanifold where the state is constant. The energy regulation controller then only operates on the energy of the periodic submanifold. This is also the main idea behind the work of [25] for inducing limit cycles in springy robots. Our control method does not require the explicit identification of these submanifolds, which can be difficult for passive locomotive systems. The disadvantage of assuming the implicit existence of these submanifolds/limit cycles through the total energy is that multiple periodic orbits can exist in the same energy level set for a $n > 2$ dimensional system. This means that in general, convergence to a reference energy does not guarantee convergence to a desired limit cycle. However, there are several examples of previous work on hybrid locomotive systems [13, 15, 24, 26, 27] that demonstrate that achieving the desired energy does achieve a desired limit cycle in practice.

2.2.2 Regulating a Varying Reference Energy

It is possible to consider a non-constant reference energy $E_{\text{ref}}(q,\dot{q},t)$ that varies with state and time. However, achieving a control that ensures the convergence of the system to $E = E_{\text{ref}}(q,\dot{q},t)$ is essentially equivalent to the steps of applying energy shaping then energy regulation as we did in the previous section. First, define an energy/Hamiltonian function $\widetilde{E} = E - E_{\text{ref}}(q,\dot{q},t)$. Then, use the Legendre transformation to derive the associated Lagrangian $\widetilde{\mathcal{L}}$, assuming that the transformation is well-defined. Finally, obtain the target dynamics through the EL equation and use the Controlled Lagrangians technique to arrive at an energy shaping control (because of this more general form of E_{ref}, more general matching conditions from [9] must be satisfied). If the reference energy has some constant term C such that $E_{\text{ref}} = f(q,\dot{q},t) + C$, it will vanish after the EL equations are applied. However, the desired convergence can be recovered by applying an outer-loop energy regulating control with $\widetilde{E} = E - f(q,\dot{q},t)$ and $E_{\text{ref}} = C$. This two step procedure allows us to clearly interpret the effect of the control as determining the shape of an energy level set through the shaping step and then stabilizing the set through energy regulation, similar to [7]. Directly regulating a time-state varying reference energy results in a less clear effect.

2.3 Application to Hybrid Locomotive Systems

Our main interest in this paper is to use energy shaping control to match the closed-loop dynamics to a passive locomotive system. This is what allows us to bypass the issue of explicitly identifying a coordinate transformation or submanifold in the state space. These systems generally have limit cycles that depend on the value of their parameters [17, 21], meaning that we can generate new cycles by changing those parameters in the virtual system. The basin of attraction of these limit cycles are typically small, hence we will use energy regulation to increase the basin in order to make gait transitions more robust as shown in [13]. This method of gait transition is basically the idea of Lyapunov funneling, see [18, 19]. However, the hybrid nature of the dynamics can present conceptual challenges to the application of both energy shaping and regulation control methods.

If the impact map Δ depends on the system parameters and we are limited only to continuous/non-impulsive control, then we are unable to completely emulate arbitrary virtual hybrid systems. This idea is related to work on energy shaping and Controlled Symmetries [28], of which a key component was demonstrating that the impact dynamics of a rigid biped are invariant with respect to the ground slope parameter. However, it is completely possible to change the virtual parameters of only the closed-loop continuous dynamics, while using the original open-loop impact dynamics. We expect that the qualitative relationship between gait characteristics (e.g., walking speed) and parameters will be similar between the true system and partially emulated virtual system, and we are not aware of any previous work that has considered this approach.

The impact map also influences the construction of an energy regulating control. If a passive walker has a conserved energy on its periodic orbit in the continuous dynamics, then the energy must be conserved across the discrete dynamics as well. This implies an equilibrium between the kinetic energy lost from dissipative impact and the potential energy gained from shifting the world frame [29]. This equilibrium can be unstable, such that a small perturbation will cause the impact dynamics to drive the energy away from the limit cycle [17]. However, it could be possible to use energy regulation to stabilize these passively unstable limit cycles. The idea is that over the flow of the continuous dynamics, the energy regulating controller compensates for the destabilizing effect of the impact dynamics. Consider the step to step storage function

$$S_{i+1}^- = \int_0^{t_i} (\dot{q}^\top B u_r)(E - E_{\text{ref}})\, d\tau + S_i^+ \tag{17}$$

$$= \int_0^{t_i} (\dot{q}^\top B u_r)(E - E_{\text{ref}})\, d\tau + \Delta_S(q^-, \dot{q}^-) + S_i^- \tag{18}$$

$$\tag{19}$$

where t_i is the time between impacts and Δ_S is the change in

the storage function at impact. If

$$0 \geq \int_0^{t_i} (\dot{q}^\top B u_r)(E - E_{\text{ref}})\, d\tau + \Delta_S(q^-, \dot{q}^-) \qquad (20)$$

then $S_{i+1}^- \leq S_i^-$, meaning the storage function is always decreasing between impacts and the energy is converging to the target energy. This is basically the notion of a hybrid storage function and so-called "jump and flow passivity" [30], but applied to orbital stabilization. For an unstable passive limit cycle, $\Delta_S > 0$, while a stable one corresponds to $\Delta_S < 0$. From equation (15), the amount of storage dissipated over the continuous dynamics can be modulated with the gain κ. Again, even if the inequality (20) is satisfied and the reference energy is asymptotically stable, this is only a necessary but not sufficient condition for achieving a limit cycle in general. Furthermore, this leaves the method of finding the E_{ref} associated with the equilibrium point induced by the impact dynamics as an open question. At the end of the next section, we offer an adaptive discrete update law to accomplish this online for a hopping robot.

3 A Hopping Robot

This section considers a simple model of a hopping robot with 1 degree-of-freedom (DOF). This makes it easier to offer analytical proofs of stability due to the linear continuous dynamics and low dimensionality. Some of the information on the passive dynamics is similar to other works on hoppers [20] and the rimless wheel [31]. The model serves as a simple non-abstract example to demonstrate and develop our ideas for application to the SLIP and compass gait models later in the paper. The novelty in this section is: 1) the analytical procedure of using energy shaping and regulation to achieve desired limit cycle characteristics, 2) proof of stabilization of a range of limit cycles using energy shaping and regulation, and 3) a discrete update law for the reference energy to deal with unknown environments.

3.1 Hopper Dynamics

Consider an actuated mass-spring system hopping on a static flat surface and constrained to move along the vertical axis. The continuous dynamics has two phases/equations

$$\textbf{Stance (ST)} \quad u = m\ddot{y} + k(y - y_0) + mg \qquad (21)$$

$$\textbf{Flight (FL)} \quad 0 = m\ddot{y} + mg \qquad (22)$$

where the mass of the point is m, the distance from the point to the ground is y, the relaxed length of the spring is y_0, the gravitational acceleration constant is g, and the actuation force is u. The discrete dynamics that govern the switch between these phases are

$$\text{if} \quad \textbf{phase} == \textbf{FL} \quad \text{and} \quad y \leq y_c \qquad (23)$$
$$\dot{y}^+ = e\dot{y}^-$$
$$\textbf{phase} := \textbf{ST}$$
$$\text{if} \quad \textbf{phase} == \textbf{ST} \quad \text{and} \quad y \geq y_0 \qquad (24)$$
$$\textbf{phase} := \textbf{FL}$$

where the superscripts - and + indicate pre-impact and post-impact states, respectively. The spring length at impact is y_c, and e is the coefficient of restitution. If $e = 1$, the impact is elastic, and if $0 < e < 1$, the impact is plastic. The switch from stance to flight at $y \geq y_0$ occurs because the ground is a unilateral constraint that cannot pull the mass into the ground, but rather can only push it away. For this reason, we only consider a relaxed or pre-compressed spring $y_c \leq y_0$ at impact. We note that this exact model might be difficult to physically realize; it serves as simple abstract template for a hybrid Lagrangian system with periodic motion.

3.2 Hopper Passive Dynamics

Periodic orbits in Lagrangian systems necessarily have a conserved energy, which implies the system energy must be conserved at impact. For periodic orbits of the passive hopper, this means the energy added by the spring pre-compression must equal the energy dissipated by the impact with

$$\frac{1}{2}k(y_0 - y_c)^2 = \frac{1}{2}m(1-e)^2(\dot{y}^-)^2. \qquad (25)$$

If the impact is plastic, then the orbit can be shown to be locally exponentially stable in the sense of Lyapunov by considering the energy state from impact to impact. Before impact,

$$E_i^- = \frac{1}{2}m(\dot{y}^-)^2 + mgy_c, \qquad (26)$$

and after

$$E_i^+ = \frac{1}{2}m(e\dot{y}^-)^2 + \frac{1}{2}k(y_0 - y_c)^2 + mgy_c. \qquad (27)$$

Since energy is conserved over the continuous dynamics, $E_i^+ = E_{i+1}^-$, which implies that

$$E_{i+1}^- = e^2 E_i^- + \frac{1}{2}k(y_0 - y_c)^2 + (1 - e^2)mgy_c. \qquad (28)$$

Because $0 < e < 1$, this discrete system is exponentially stable and

$$E \to \frac{k(y_0 - y_c)^2}{2(1 - e^2)} + mgy_c = E_{\text{lim}}. \qquad (29)$$

This forms an analytical Poincaré map [2], thus there is always a locally exponentially stable hybrid limit cycle for the hopper.

For all parameter cases of the passive hopper, the system will get stuck in the stance phase if the energy is too low to achieve liftoff. In addition, the mass can bottom out against the ground if the energy is too large, which we consider to be a system failure. This implies that basin of attraction is bounded by these two energy level sets as

$$mgy_0 < E < \frac{1}{2}ky_0^2. \tag{30}$$

If $e = 1$ and $y_c = y_0$, the energy is always conserved across all dynamic regimes and there is a family of marginally stable periodic orbits within these energy bounds.

3.3 Hopper Control

The hopping height y_{apex} is limited by the upper bound on the energy with the expression

$$y_{\text{apex}} < \frac{ky_0^2}{2mg}. \tag{31}$$

The good news is that energy shaping can be used to change the virtual spring stiffness $\widetilde{k}$ to increase the basin ceiling and achieve arbitrary hopping heights, while energy regulation can be used to create energy for liftoff and minimize the basin floor. The resulting control and closed loop stance dynamics are

$$u = u_s + u_r \tag{32}$$
$$= (k-\widetilde{k})(y-y_0) - \kappa(\widetilde{E} - E_{\text{ref}})\dot{y} \tag{33}$$
$$0 = m\ddot{y} + \kappa(\widetilde{E} - E_{\text{ref}})\dot{y} + \widetilde{k}(y-y_0) + mg \tag{34}$$

where $\widetilde{E} = \frac{1}{2}m\dot{y}^2 + \frac{1}{2}\widetilde{k}(y-y_0)^2 + mgy$. If there is a linear damping term in the stance dynamics $d\dot{y}$, it acts as a shift on the reference energy as $E_{\text{new}} = E_{\text{ref}} - \frac{d}{\kappa}$ so the damped hopper system can be addressed by this example as well. Interestingly, the new stance dynamics correspond exactly to the *harmonic* Rayleigh-Van-der-Pol oscillator from [32] (which we elaborate on in the following section on the SLIP model).

In the case of $e = 1$ and $y_c = y_0$, we can choose any reference energy that satisfies equation (30) to achieve a virtual passive limit cycle. In the case of $0 < e < 1$ and $0 < y_c < y_0$, we must choose E_{ref} to be exactly equal to equation (29) if we want to ensure that the hopping limit cycle mimics a passive system. Consider the step-to-step storage function at impact,

$$S_i^+ = \frac{1}{2}(E^+ - E_{\text{ref}})^2 \tag{35}$$
$$= \frac{1}{2}(e^2E_i^- + \frac{1}{2}k(y_0-y_c)^2 - E_{\text{ref}})^2. \tag{36}$$

If $0 < e < 1$ and $E_{\text{ref}} = E_{\text{lim}}$, then $S_i^+ = e^4S_i^-$ and the storage function decreases after impact, i.e., $S_i^+ \leq S_i^-$. The energy regulation control causes the storage to decrease over the continuous dynamics, implying $S_{i+1}^- \leq S_i^+$. It follows then that $S_{i+1}^- \leq S_i^-$; the post impact storage function monotonically decreases from event to event. Thus, the hybrid limit cycle of the system under the energy regulation control is asymptotically stable.

One could expect a hopping robot to operate in different environments with varying coefficients of restitution that cannot be estimated before hand. So it would be useful in practice to have a method of updating E_{ref}. Inspired by structure of the impact dynamics, we propose the update policy

$$E_{\text{ref}_{i+1}} = E_{\text{ref}_i} + \lambda(E_i^+ - E_i^-). \tag{37}$$

where λ is a scaling gain. Essentially, if the impact dynamics cause a net gain in E then E_{ref} is increased, and vice-versa. From the convergence of S in the continuous dynamics, $|E_{i+1}^- - E_{\text{ref}_i}| \leq |e^2E_i^- - E_{\text{ref}_i}|$. Though some manipulation, this can be converted into the form

$$\begin{bmatrix} E_{\text{ref}_{i+1}} \\ E_{i+1}^- \end{bmatrix} = \begin{bmatrix} 1 & \lambda(e^2-1) \\ c & d \end{bmatrix} \begin{bmatrix} E_{\text{ref}_i} \\ E_i^- \end{bmatrix} + B \tag{38}$$
$$= A \begin{bmatrix} E_{\text{ref}_i} \\ E_i^- \end{bmatrix} + B \tag{39}$$

where B is a constant, and $|c+d| < 1$. Then from the Perron-Frobenius theorem [33], the maximum absolute eigenvalue of A is less than one if $|1+\lambda(e^2-1)| < 1$. Therefore, this update law is globally stable for $-1 < \lambda < 0$ and the reference energy will converge to the energy of the passive limit cycle.

This update law can generalize to higher dimensional systems, which we show through numerical simulation on the compass gait biped in a later section. We remark that in practice, using a different constant value of E_{ref} can still result in a limit cycle as in [20], but the asymptotic trajectory will not emulate a virtual passive system and is dependent on the value of the gain κ. Finally, the proof of stability for the hopper system relies on the stability properties of the passive limit cycle, $0 < e < 1$. This leads us to believe that in general, the energy associated with an unstable limit cycle cannot be arrived at via (37).

4 Spring Loaded Inverted Pendulum

The SLIP model can be considered as an extension of the hopping robot that exhibits behaviors and properties similar to human walking and running [21]. It comprises a point mass that moves via connecting the mass to the ground through ideal springs. The version we consider here has 2-DOF, can exhibit both walking and running behaviors, and has additional control actuation along the spring axis. The walking behavior alternates between a single support phase

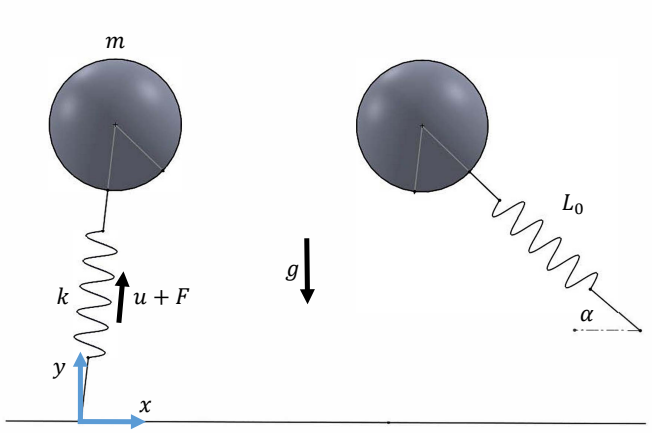

Fig. 1. Diagram of the spring loaded inverted pendulum.

and a double support phase, while the running behavior alternates between a single support phase and a flight phase. In this paper, we consider only the running behavior for simplicity. A diagram of the model is given in Fig. 1. The primary novelty of this section is using energy regulation based methods to achieve dynamic gait transitions in the SLIP model.

4.1 SLIP Dynamics and Control

In general, the energy of the system is

$$E = \mathcal{K}(\dot{q}) + \mathcal{P}(q) \tag{40}$$

$$= \frac{1}{2}m(\dot{x}^2 + \dot{y}^2) + \frac{1}{2}k(L(x,y) - L_0)^2 + mgy \tag{41}$$

The configuration vector of the model is $q = [x,y]^\top$, the point mass is m, and the length and stiffness of the springs are L and k, respectively. The gravitational acceleration constant is g, and is along the vertical coordinate y. At the relaxed spring length $L = L_0$ the system releases the spring from the ground, and it engages the spring again at the contact angle α when $y = L\sin(\alpha)$. The rules for releasing and engaging the spring ensure that the spring energy is zero at phase transitions, thus the energy of the open-loop system is conserved across all regimes. The switching rules and the EL equation lead to the following equations of motion:

$$\textbf{Stance (ST)} \quad Ju = M\ddot{q} + G \tag{42}$$

$$\textbf{Flight (FL)} \quad 0 = M\ddot{q} + \begin{bmatrix} 0 \\ mg \end{bmatrix} \tag{43}$$

$$\text{if} \quad \textbf{phase} == \textbf{FL} \quad \text{and} \quad y \le L_0\sin(\alpha) \tag{44}$$

$$\quad \textbf{phase} := \textbf{ST}$$

$$\text{if} \quad \textbf{phase} == \textbf{ST} \quad \text{and} \quad L \ge L_0 \tag{45}$$

$$\quad \textbf{phase} := \textbf{FL}$$

The matrix J maps the control input u (collinear with the spring forces) into the stance coordinates. The system is underactuated with degree 1 during the single support phase and has no continuous actuation during the flight phase, though we claim control authority over the touchdown contact angle α.

In [21], it is shown that for a constant spring stiffness k and touchdown angle α, there is a compact set of energies that correspond to walking or running periodic orbits in the SLIP model. They also show that these energy sets exist and change for a range of stiffnesses and touchdown angles. This is our motivation to use energy shaping to change the spring stiffness. Because the energy of the open-loop system is conserved, any periodic orbit is only marginally stable. Thus, it is reasonable to use energy regulation to stabilize the orbit. However, because the SLIP model has a 4 dimensional state space instead of the 2 dimensional space of the hopper, a single energy value does not uniquely define a trajectory of the open-loop system. Additionally, work in both [21] and [34] indicates that controlling the contact angle is critical to the stability of this model. Inspired by [34], we use the policy

$$\alpha_{i+1} = \frac{1}{2}(\alpha_i + \pi - \theta_i) \tag{46}$$

to update the contact angle, where θ_i is the take off angle. This policy reaches an equilibrium when the touchdown and liftoff positions are symmetric about the y axis.

The control is partitioned into $u = u_s + u_r$. The stiffness change is accomplished with $u_s = (k - \widetilde{k})(L - L_o)$. Using the storage function of equation (9), the time derivative under the SLIP dynamics is

$$\dot{S} = (\widetilde{E} - E_{\text{ref}})\dot{q}^\top J u_r \tag{47}$$

which means we should choose

$$u_r = -\kappa\dot{L}(\widetilde{E} - E_{\text{ref}}) \tag{48}$$

to ensure that $\dot{S}$ is negative semi-definite.

In section 3.3 we mentioned that the energy regulation control caused the closed-loop hopper system to take the form of a harmonic Rayleigh-Van-der-Pol oscillator. By inserting these closed loop dynamics into the SLIP model, we can examine the effect of the "unmodeled" rotational dynamics around the spring contact point. The motivation is that this will be suggestive of qualitative behavior of embedding this energy regulated SLIP model into higher order biped models as in [15] without aggressive compensation of dynamics transverse to the spring action. The recycling of the 1-DOF hopper controller for the SLIP model is accomplished by using only the energy of the SLIP model along the spring axis as

$$u_r = -\kappa\dot{L}(\frac{1}{2}m\dot{L}^2 + \frac{1}{2}\widetilde{k}(L - L_0)^2 - E_{\text{ref}}). \tag{49}$$

The potential benefit of controller (49) over (48) is that it requires less state information, but with the drawback that the limit cycle trajectory will certainly not emulate a passive system.

4.2 SLIP Simulations

This section offers simulation results that demonstrate the ability to use energy shaping regulation methods to achieve different running speeds on the SLIP model. The control in equation (48) is termed the regulation control while equation (49) is termed the oscillator control. We started with an initial known running gait from [34], with $m = 70$ kg, $L_o = 1$ m, $\alpha = 55°$, $\widetilde{k} = k = 8200\frac{N}{m}$, and $E = 1860J$ (marked as a red dot in Fig. 2-6). For all cases, $\kappa = 1$. For the oscillator, we heuristically found a reference energy value $E = 583J$ that resulted in an average speed similar to the known gait ($\approx 6\frac{m}{s}$). We created a grid of target energies and stiffnesses around this configuration, used the flight apex of the known gait as the initial condition for every grid point, and allowed the system to converge to a new limit cycle. This means that every stable grid point is a stable transition from the initial limit cycle to a new limit cycle due to a single change in reference energy and/or virtual stiffness. The existence and stability of the limit cycle were confirmed via the numerical linearization of the Poincaré return map via the method from [2].

The results for the stable average running speed of the model under the energy shaping and regulation control and the embedded harmonic Rayleigh-Van-der-Pol oscillator are given in Fig. 2 and 4. The edge of each surface indicates the edge of the sampling grid, or a case where the model fell through the floor or went backwards. For the regulation control in Fig. 2, the speed level set projections indicate that stiffness does not determine the average speed which agrees with the results of [21] that show a range of walking speeds for a given spring stiffness. However, the oscillator control causes a qualitative change in this relationship so that the average speed does depend on stiffness and reference energy as seen in Fig. 4. The two methods give a similar range of achievable walking speeds. We emphasize again that these new gaits are all the result of stable transitions from the passive known gait. A sample trajectory for the energy regulation controller is given in Fig. 3, where the known gait is run for 3 steps then the parameters are switched and the trajectory and contact angle converge to a new gait.

Plots of the equilibrium contact angle as a function of stiffness and energy are given in Fig. 5 and 6 for direct comparison to the results in [21]. Both methods have a similar range of contact angles; the difference between them is largely that the embedded oscillator surface in Fig. 6 seems to be flatter than the surface in Fig. 5. This indicates that there might be some constant normal vector in this space associated with stability for the system under the embedded oscillator.

The most important take away from these simulation results is that a single change in parameters using energy shaping and regulation can achieve a stable transition between fast and slow running. Also, the principles of energy shaping and regulation control can be applied to a subcomponent of the system to achieve qualitatively similar behavior. We expect that this could be extremely useful in the application of these methods to wearable devices to assist locomotion, like a powered prosthesis [35] or orthosis [36], where measuring the total energy of the combined human-robot system is infeasible.

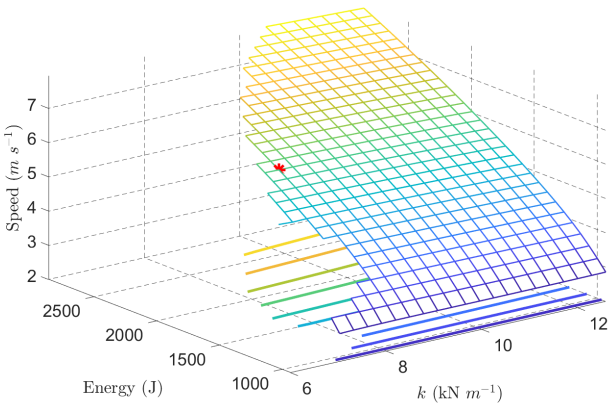

Fig. 2. Speed-Energy-Stiffness surface for the SLIP model under the regulation control. The minimum speed achieved was $2.82\frac{m}{s}$, the maximum $7.95\frac{m}{s}$.

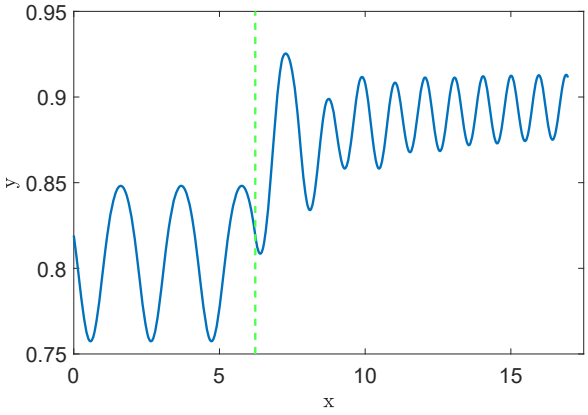

Fig. 3. Sample trajectory of transition from $6\frac{m}{s}$ to $3\frac{m}{s}$ under the regulation control. The stiffness and reference energy were switched at the horizontal dashed line.

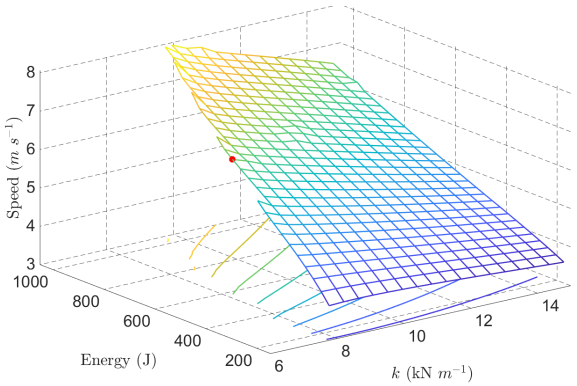

Fig. 4. Speed-Energy-Stiffness surface for the SLIP model under the oscillator control. The minimum speed achieved was $3.65\frac{m}{s}$, the maximum $8.05\frac{m}{s}$.

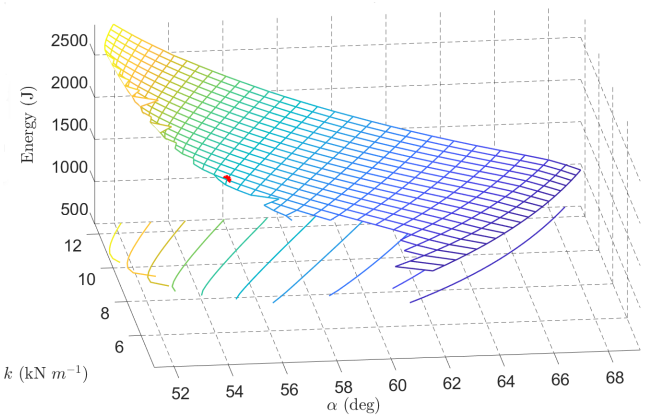

Fig. 5. Contact Angle-Energy-Stiffness surface for the SLIP model under regulation control.

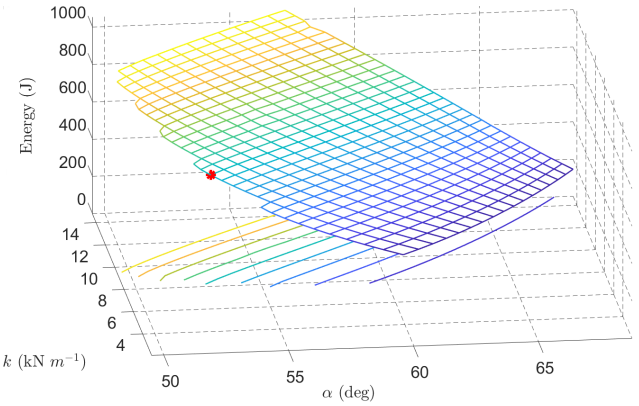

Fig. 6. Contact Angle-Energy-Stiffness surface for the SLIP model under the oscillator control.

5 Compass Gait Biped

The compass gait biped can walk down a shallow slope under the power of gravity alone by reaching an energy equilibrium between the potential energy gained and the kinetic energy lost at each impact [17]. Much of the research in the control of dynamic biped locomotion uses this model as a testbed, to the point some have titled it "The Simplest Walking Model" [22]. Similar to the SLIP model, different walking speeds emerge for a given set of system parameters [17], which motivates the application of the energy shaping and regulation control methods. A diagram of the model is given in Fig. 7.

5.1 Compass Gait Biped Dynamics and Control

The biped undergoes an instantaneous rigid impact when the swing leg hits the ground. The impact model from [2] and the EL equation gives the following hybrid dynamics for the compass gait biped:

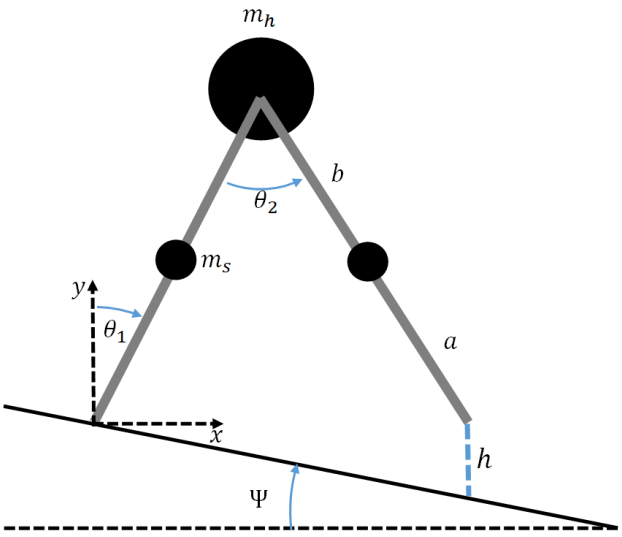

Fig. 7. Diagram of the compass gait biped. The legs are symmetric.

$$M(q)\ddot{q}+C(q,\dot{q})\dot{q}+G(q)=u \tag{50}$$

$$\begin{bmatrix}\dot{q}^+\\ F_I\end{bmatrix}=R\begin{bmatrix}M & -A^\top\\ A & 0_{2x2}\end{bmatrix}^{-1}\begin{bmatrix}M\\ 0_{2x2}\end{bmatrix}\dot{q}^- \quad \text{if } h(q,\Psi)\le 0$$
$$q^+=Rq^-. \tag{51}$$

The continuous dynamics are described by (41), where $q=[\theta_1,\theta_2]^\top$, M is the mass matrix, C is the corriolis/centrifugal matrix, $G=\frac{\partial \mathcal{P}(q)}{\partial q}$ is the gravity vector, and u is the vector of control torques applied at the joints. The discrete dynamics are described by (51). They have a plastic impact map that depends on M, a matrix A that describes the constraint of the impact foot to the ground, and a relabeling matrix R that swaps the swing and stance legs. The impact maps a pre-impact velocity vector $\dot{q}^-$ to a post-impact velocity $\dot{q}^+$ and an impact force F_I. The vertical distance from the swing leg to the ground is h. For additional modeling details, see [13] and [17].

Using the framework from Section 2.2, the energy shaping control is

$$u_s=-M\widetilde{M}^{-1}(\widetilde{C}\dot{q}+\widetilde{G})+C\dot{q}+G \tag{52}$$

while the energy regulation control is

$$u_t=-\kappa(\widetilde{E}-E_{\text{ref}})M\widetilde{M}^{-1}\Omega\dot{q} \tag{53}$$

The closed-loop dynamics are then

$$\widetilde{M}\ddot{q}+(\widetilde{C}+\kappa(\widetilde{E}-E_{\text{ref}})\Omega)\dot{q}+\widetilde{G}=0. \tag{54}$$

The parameters available for shaping in the energy function of the system are: $\widetilde{m}_h,\widetilde{m}_s,\widetilde{a},\widetilde{b}$ and $\widetilde{g}$. The question then

becomes: how should we choose these values? In [37], the effect of gravity shaping on the compass gait biped is thoroughly explored, indicating that average walking speed is proportional to $\sqrt{\widetilde{g}}$. In [17], it is shown that the dynamics can be normalized to depend on the mass ratio $\mu = \frac{m_h}{m_s}$ and the length ratio $\beta = \frac{b}{a}$, which both influence the average speed. Because the impact dynamics depend only on M, we can exactly emulate a target $\widetilde{g}$ but we cannot do the same for $\widetilde{\beta}$ and $\widetilde{\mu}$. This means we could exactly reproduce the results from [37] in the closed-loop hybrid dynamics, but we cannot change $\widetilde{\mu}$ and $\widetilde{\beta}$ to reproduce similar results from [17]. The primary novelty of this section is the exploration of the relationship between the walking speed and a virtual change in $\widetilde{\mu}$ and $\widetilde{\beta}$ during the continuous dynamics while using the natural values in the impact dynamics. In addition, we show that energy regulation can be used to stabilize period-1 gaits that otherwise would go unstable and bifurcate as mass parameters vary [17].

In the hopper with plastic impacts, we were able to analytically compute the E_{ref} for a given passive limit cycle using equation (29). In general, it is not possible to know the energy of a passive biped limit cycle without simulating it numerically. This poses a challenge to dynamically changing the virtual parameters and reference energy to achieve new passive limit cycles without making a library of precomputed gaits. In [26], a discrete step-by-step update law for E_{ref} in an energy regulation control is proposed, as

$$E_{\text{ref}_{i+1}} = E_{\text{ref}_i} + \lambda(v_{\text{ref}} - v_i). \tag{55}$$

This law achieves a desired average walking speed v_{ref}, where λ is a scaling gain and v_i is the average walking speed for the i_{th} step. However this law simply shifts the problem to picking the v_{ref} associated with a natural limit cycle before hand, instead of E_{ref}. Instead, we can reuse the update law in equation (37) from the 1-DOF hopper and apply it to the compass gait biped. A comparison between these strategies on a simulated biped is given in the following section. We use u^{nat} to denote the control under equation (37) and u^{vel} for equation (55).

5.2 Compass Gait Biped Simulations

We now present simulation results for the compass gait biped under the energy shaping and regulation controls. The baseline parameters we use are $m_h = 10\text{kg}, m_s = 5\text{kg}, a = 0.5\text{m}, b = 0.5\text{m}, \Psi = 3.7^\circ$ with a known initial condition for a stable limit cycle from [17]. We compare changes in the true ratios β against changes in the virtual ratios $\widetilde{\beta}$ during the continuous dynamics. We omit results for μ and $\widetilde{\mu}$ for brevity. The energy regulation controls u_t^{vel} and u_t^{nat} are applied to the system with the virtual ratios, using the control parameters $\lambda = 0.5$, $\kappa = 100$, and $\Omega = \text{diag}([1,0])$. Each reference velocity v_{ref} for a given ratio is taken from the corresponding physical ratio limit cycle. The ratios that we sample are on a uniform grid from 0.5 to 1, and we do not display data points in the grid range that either bifurcated or were unstable within our search tolerance. We confirm the stability of the limit cycles using the linearized Poincaré return map.

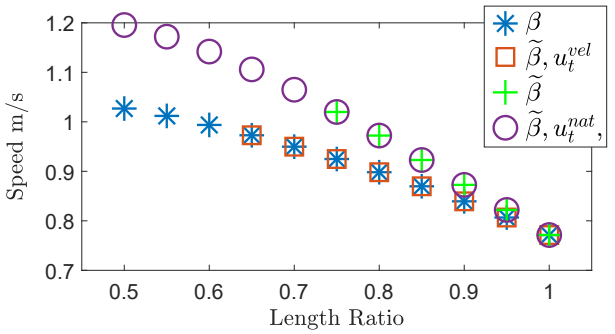

Fig. 8. Length ratio versus average speed for physical and virtual dynamics. β is the physical length ratio, $\widetilde{\beta}$ is the virtual length ratio, u_t^{vel} converges to a desired walking speed, u_t^{nat} converges to the energy equilibrium induced by the discrete dynamics. Data points that bifurcated or were unstable are not displayed.

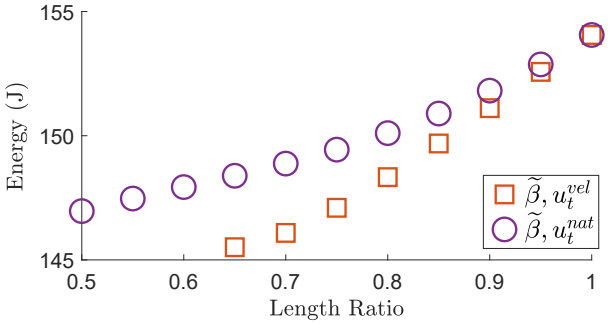

Fig. 9. Energy versus length ratio for the adaptive energy regulation controllers. Data points that bifurcated or were unstable are not displayed.

The results are shown in Figs. 8, 9, and 10. We can see that shaping the continuous dynamics alone through $\widetilde{\beta}$ does not reproduce the same limit cycle as physically changing the parameters. In Fig. 8, the virtual length ratio $\widetilde{\beta}$ has the same general trend between ratio and speed as β, but it causes a larger increase in walking speed. The introduction of u_t^{nat} enables E_{ref} to converge to $\widetilde{E}_{\text{nat}}$, as evidenced where the circle and cross data points overlap in the figures. It also increases the range of achievable speeds, as seen by the circle data points that do not overlap the cross points. The velocity update law u_t^{vel} causes the shaped system to converge to the targeted walking speed of the associated physical system, as seen by the overlap of the squares and stars. Fig. 9 shows the energies that the update laws converge to, indicating the real parameters shift energy down more than the virtual ones. In Fig. 10, we can see that u_t^{vel} causes limit cycles that are less efficient compared to those from u_t^{nat}, in the sense that they require more torque output from the control to achieve the same walking speed. These inefficient cycles are due to the fact that they are unnatural and must compensate for the energy mismatch between $\widetilde{E}_{\text{ref}}$ and $\widetilde{E}_{\text{nat}}$.

Finally, we offer a simulation example of using energy regulation to stabilize an unstable limit cycle. In this case, the terrain is changed from a slope to stairs of a similar ge-

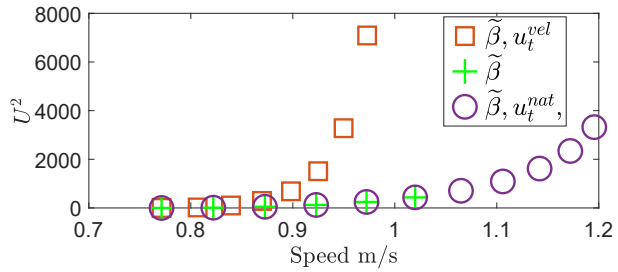

Fig. 10. Time integral of torque squared versus average speed for physical and virtual dynamics length ratio changes. Data points that bifurcated or were unstable are not displayed.

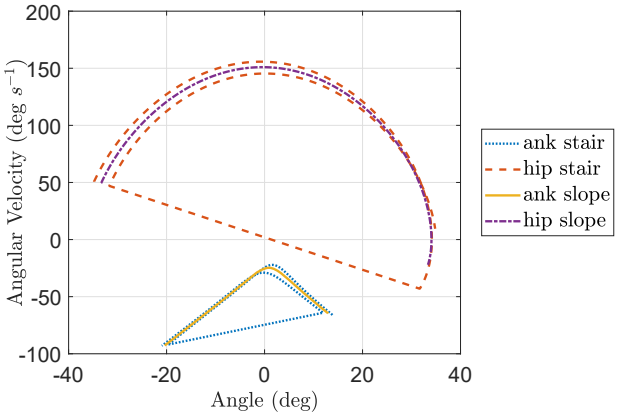

Fig. 11. The slope period-1 passive limit cycle versus the stairs period-2 passive limit cycle.

ometry. Thus, the impact map $\Delta(q, \dot{q})$ remains the same but the switching surface $\mathbf{S}$ and distance function h are changed. The stair impact map still admits the energy equilibrium from the slope dynamics, however as seen in Fig. 11 this is not associated with a stable period-1 limit cycle for the passive system. In Fig. 12, we present a stair walking simulation where we switch on the energy regulation control after 4 steps and run it for 10 more steps. This causes the biped to converge to the period 1 slope limit cycle while walking on the stairs terrain, indicating that we have stabilized this previously unstable gait.

6 Conclusion

In this article we have explored some principles and extensions of energy shaping and regulation control for generating and transitioning between limit cycles in simple locomotive systems. We analytically and numerically demonstrated that energy regulation can increase the basin of attraction of the limit cycle so that parameter switches in an energy shaping control lead to stable gait transitions in a trajectory-free manner. Our contributions are: 1) the demonstration of the equivalence between the 2-step process of energy shaping then energy regulation, and regulation of time and state varying energy functions, 2) a discrete update law for E_{ref} to allow convergence to a passive limit cycle online, 3) transitioning between running gaits on the SLIP model, 4) a novel examination of energy shaping on the compass gait biped, 5)

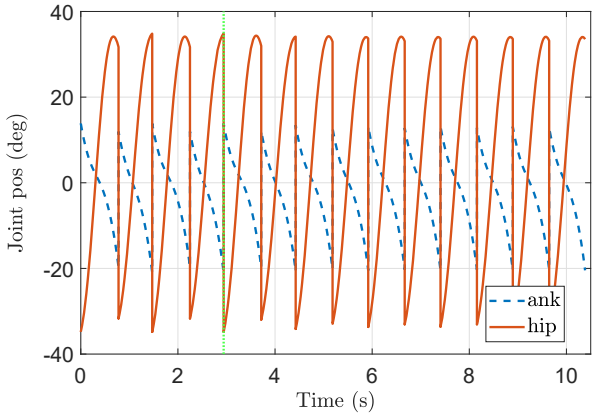

Fig. 12. Transition from passive period-2 limit cycle to an energy regulated period-1 limit cycle. The energy regulation control is turned on after 4 steps, at the green vertical line.

a theoretical explanation for using energy regulation to stabilize unstable limit cycles and demonstration on the compass gait biped. This paper also serves to connect and streamline previous works in the areas of orbital stabilization and hybrid locomotive systems. The outcome of our work here is a model with gaits based on continuously varying spring stiffness and nonlinear damping in the form of energy regulation and is similar in spirit to previous work on variable impedance control for a powered prosthesis [38]. As such, we plan to utilize the theory and results in this work to shape the dynamics of a powered prosthetic leg to mirror the SLIP model to aid locomotion with task variation like changing walking speeds and slopes.

Acknowledgements

This work was supported by NSF Award 1652514 / 1949869. Robert D. Gregg holds a Career Award at the Scientific Interface from the Burroughs Wellcome Fund.

References

[1] Westervelt, E. R., Grizzle, J. W., and Koditschek, D. E., 2003. "Hybrid zero dynamics of planar biped walkers". *IEEE transactions on automatic control,* **48**(1), pp. 42–56.

[2] Westervelt, E. R., Grizzle, J. W., Chevallereau, C., Choi, J. H., and Morris, B., 2007. "Feedback Control of Dynamic Bipedal Robot Locomotion". *Crc Press*, p. 528.

[3] Powell, M. J., Hereid, A., and Ames, A. D., 2013. "Speed regulation in 3d robotic walking through motion transitions between human-inspired partial hybrid zero dynamics". In 2013 IEEE international conference on robotics and automation, IEEE, pp. 4803–4810.

[4] Saglam, C. O., and Byl, K., 2015. "Meshing hybrid zero dynamics for rough terrain walking". In 2015 IEEE International Conference on Robotics and Automation (ICRA), IEEE, pp. 5718–5725.

[5] Ma, W.-L., Hamed, K. A., and Ames, A. D., 2019.

"First steps towards full model based motion planning and control of quadrupeds: A hybrid zero dynamics approach". *arXiv preprint arXiv:1909.08124*.

[6] Ortega, R., Spong, M. W., Gomez-Estern, F., and Blankenstein, G., 2002. "Stabilization of a class of undercactuated mechanical systems via interconnection and damping assignment". *IEEE Trans. Autom. Control,* **47**(8), pp. 1218–1233.

[7] Yi, B., Ortega, R., Wu, D., and Zhang, W., 2020. "Orbital stabilization of nonlinear systems via mexican sombrero energy shaping and pumping-and-damping injection". *Automatica,* **112**, p. 108661.

[8] Bloch, A. M., Leonard, N. E., and Marsden, J. E., 2001. "Controlled Lagrangians and the stabilization of Euler-Poincare mechanical systems". *International Journal of Robust and Nonlinear Control,* **11**(3), pp. 191–214.

[9] Blankenstein, G., Ortega, R., and Van Der Schaft, A. J., 2002. "The matching conditions of controlled lagrangians and ida-passivity based control". *International Journal of Control,* **75**(9), pp. 645–665.

[10] Chang, D. E., Bloch, A. M., Leonard, N. E., Marsden, J. E., and Woolsey, C. A., 2002. "The equivalence of controlled lagrangian and controlled hamiltonian systems". *ESAIM: Control, Optimization and Calculus of Variations,* **8**, pp. 393–422.

[11] Kotyczka, P., and Sarras, I., 2012. "Equivalence of immersion and invariance and ida-pbc for the acrobot". *IFAC Proceedings Volumes,* **45**(19), pp. 36–41.

[12] McCourt, M. J., and Antsaklis, P. J., 2009. "Connection between the passivity index and conic systems". *ISIS,* **9**(009).

[13] Spong, M., Holm, J., and Lee, D., 2007. "Passivity-Based Control of Bipedal Locomotion". *IEEE Rob. Autom. Mag.,* **14**(June), pp. 30–40.

[14] Gregg, R. D., and Spong, M. W., 2010. "Reduction-based control of three-dimensional bipedal walking robots". *Int. J. Rob. Res.,* **29**(6), pp. 680–702.

[15] Garofalo, G., Ott, C., and Albu-Schäffer, A., 2012. "Walking control of fully actuated robots based on the bipedal slip model". In 2012 IEEE International Conference on Robotics and Automation, IEEE, pp. 1456–1463.

[16] Sinnet, R. W., and Ames, A. D., 2015. "Energy shaping of hybrid systems via control lyapunov functions". In American Controls Conference, pp. 5992–5997.

[17] Goswami, A., Thuilot, B., and Espiau, B., 1996. "Compass-like biped robot part i: Stability and bifurcation of passive gaits". PhD thesis, INRIA.

[18] Gregg, R. D., Tilton, A. K., Candido, S., Bretl, T., and Spong, M. W., 2012. "Control and planning of 3-d dynamic walking with asymptotically stable gait primitives". *IEEE Transactions on Robotics,* **28**(6), pp. 1415–1423.

[19] Bhounsule, P. A., Zamani, A., and Pusey, J., 2018. "Switching between limit cycles in a model of running using exponentially stabilizing discrete control lyapunov function". In 2018 Annual American Control Conference (ACC), IEEE, pp. 3714–3719.

[20] Garofalo, G., and Ott, C., 2019. "Repetitive jumping control for biped robots via force distribution and energy regulation". In *Human Friendly Robotics*. Springer, pp. 29–45.

[21] Geyer, H., Seyfarth, A., and Blickhan, R., 2006. "Compliant leg behaviour explains basic dynamics of walking and running". *Proceedings of the Royal Society B: Biological Sciences,* **273**(1603), pp. 2861–2867.

[22] Garcia, M., Chatterjee, A., Ruina, A., and Coleman, M., 1998. "The simplest walking model: stability, complexity, and scaling". *Journal of biomechanical engineering,* **120**(2), pp. 281–288.

[23] Ouakad, H., Nayfeh, A., Choura, S., Abdel-Rahman, E., Najar, F., and Hammad, B., 2008. "Nonlinear feedback control and dynamics of an electrostatically actuated microbeam filter". In ASME International Mechanical Engineering Congress and Exposition, Vol. 48746, pp. 535–542.

[24] Yeatman, M., Lv, G., and Gregg, R. D., 2019. "Decentralized passivity-based control with a generalized energy storage function for robust biped locomotion". *Journal of Dynamic Systems, Measurement, and Control,* **141**(10), p. 101007.

[25] Garofalo, G., and Ott, C., 2016. "Energy based limit cycle control of elastically actuated robots". *IEEE Transactions on Automatic Control,* **62**(5), pp. 2490–2497.

[26] Goswami, A., Espiau, B., and Keramane, A., 1997. "Limit cycles in a passive compass gait biped and passivity-mimicking control laws". *Autonomous Robots,* **4**(3), pp. 273–286.

[27] Sinnet, R. W., 2015. "Energy shaping of mechanical systems via control lyapunov functions with applications to bipedal locomotion". PhD thesis, Texas A & M University.

[28] Spong, M. W., and Bullo, F., 2005. "Controlled symmetries and passive walking". *IEEE Trans. Autom. Control,* **50**(7), pp. 1025–1031.

[29] McGeer, T., et al., 1990. "Passive dynamic walking". *Int. J. Robotic Res.,* **9**(2), pp. 62–82.

[30] Naldi, R., and Sanfelice, R. G., 2013. "Passivity-based control for hybrid systems with applications to mechanical systems exhibiting impacts". *Automatica,* **49**(5), pp. 1104–1116.

[31] Coleman, M. J., Chatterjee, A., and Ruina, A., 1997. "Motions of a rimless spoked wheel: a simple three-dimensional system with impacts". *Dynamics and stability of systems,* **12**(3), pp. 139–159.

[32] Nathan, A., 1977. "The rayleigh-van der pol harmonic oscillator". *International Journal of Electronics Theoretical and Experimental,* **43**(6), pp. 609–614.

[33] Pillai, S. U., Suel, T., and Cha, S., 2005. "The perron-frobenius theorem: some of its applications". *IEEE Signal Processing Magazine,* **22**(2), pp. 62–75.

[34] Heim, S., and Spröwitz, A., 2019. "Beyond basins of attraction: Quantifying robustness of natural dynamics". *IEEE Transactions on Robotics*.

[35] Quintero, D., Villarreal, D. J., Lambert, D. J., Kapp, S., and Gregg, R. D., 2018. "Continuous-phase control

of a powered knee–ankle prosthesis: Amputee experiments across speeds and inclines". *IEEE Transactions on Robotics,* **34**(3), pp. 686–701.

[36] Lv, G., Zhu, H., and Gregg, R. D., 2018. "On the design and control of highly backdrivable lower-limb exoskeletons: A discussion of past and ongoing work". *IEEE Control Systems Magazine,* **38**(6), pp. 88–113.

[37] Xu, C., Ming, A., and Chen, Q., 2014. "Characteristic equations and gravity effects on virtual passive bipedal walking". In 2014 IEEE International Conference on Robotics and Biomimetics (ROBIO 2014), IEEE, pp. 1296–1301.

[38] Mohammadi, A., and Gregg, R. D., 2019. "Variable Impedance Control of Powered Knee Prostheses Using Human-Inspired Algebraic Curves". *Journal of Computational and Nonlinear Dynamics,* **14**(10), 09. 101007.